

Simulation studies on compensation for space-charge-induced half-integer and 3rd-order resonance crossing in HIAF-BRring

C.Guo,^{1,2} J.Liu,^{1,2} J.C.Yang,^{1,2,*} and R.H.Zhu^{1,2}

¹*Institute of Modern Physics, Chinese Academy of Sciences, Lanzhou 730000, China*

²*University of Chinese Academy of Sciences, Beijing 100049, China*

(Dated: August 27, 2024)

Space-charge-induced resonance crossing is one notable limitation of beam intensity in high-intensity synchrotrons. Beam instability occurs under the combined effects of space-charge-induced tune spread and magnetic field imperfections prevents, which limits the intensity. This paper proposes a space-charge-Twiss modification to the Resonance Driving Terms (RDTs). The new RDTs are named modified RDTs. Modified RDTs aim to describe the nonlinear particle dynamics under resonance crossing. The feasibility of the modified RDTs is demonstrated through simulations of half-integer and 3rd-order resonance crossings, using the lattice of the High Intensity Heavy-Ion Accelerator Facility Booster Ring (HIAF-BRring). The simulations illustrate that the compensation provided by the modified RDTs significantly suppresses emittance growth and reduces distortion in the phase space.

I. INTRODUCTION

Space charge effect is the key limitation of beam intensity in high intensity synchrotrons. It can lead to undesired beam emittance growth, beam halo formation and particle loss. Since particles with different betatron amplitudes have different betatron tune shifts, $\Delta v_{sc}(J_{x,y})$, the space charge force produces a incoherent tune spread. As the beam intensity gets stronger, the tune spread becomes larger, which would eventually lead to resonance crossing. Besides, the variation of the tunes through the synchrotron motion due to the longitudinal dependency of space charge and chromatic effects leads to periodic resonance crossing. The space-charge-induced resonance crossing has been identified as the main beam degradation mechanism in Proton Synchrotron (PS) and the Super Proton Synchrotron (SPS) at CERN[1].

Here are 4 approaches that have been proposed to mitigate this issue. Adrian Oeftiger et al. proposed a novel space charge compensation concept, pulsed electron lenses. This technique aims to mitigate the ion space charge effect through the electronic space charge effect. Simulations of the Facility for Antiproton and Ion Research (FAIR) SIS100 synchrotron demonstrated that this method could achieve up to a 30% increase in maximum beam intensity [2]. Hideaki Hotchi et al. at Facilities at Japan Proton Accelerator Research Complex (J-PARC) proposed a novel method of transverse injection painting to counteract the emittance exchange caused by Montague resonance. The beam stability was achieved by sextupole compensation under resonance crossing of 3rd-order resonance lines. However, the scheme for achieving this compensation in the rapid cycling synchrotron (J-PARC-RSC) was not demonstrated in the cited reference[3]. Meanwhile, the compensation scheme in the Main Ring (J-PARC-MR) was demonstrated in [4]. One scheme in this paper references the scheme of J-PARC-MR. Andrea Santamaria Garcia and Foteini Asvesta et al. achieved the beam stability under

resonance crossing of a half-integer resonance line by scanning currents of quadrupole correctors at Proton Synchrotron Booster[5, 6].

In these work, Resonance Driving Terms (RDTs[7]) play an important role in resonance compensation. RDTs focus on identifying and quantifying the effects of specific perturbations that could induce resonant behavior of the beam. These perturbations include imperfections in the magnetic fields of the accelerator. The Hamiltonian of the system could be expressed as a series of Fourier coefficients depending on the amplitude and phase of the beam oscillations[8]. In addition, RDTs from space charge potential were carried out in [9]. However, RDTs do not consider the influence of space charge on Twiss, which causes that RDTs do not have a good performance on compensating for magnetic field imperfections under space-charge-induced resonance crossing.

The key idea of this paper is the introduction of space-charge-Twiss modification in RDTs. This idea was verified through simulations performed on a dedicated accelerator collective instability platform, CISP[10], using the lattice of the High Intensity heavy-ion Accelerator Facility Booster Ring (HIAF-BRring[11]). In the simulations, non-structural half-integer and 3rd-order resonance lines were crossed due to the space charge incoherent tune spread. Magnetic field errors were introduced to drive corresponding resonances. The modified RDTs were then used to calculate the strength of magnetic correctors in order to compensate for these errors. For comparison, 2 additional compensation schemes were also demonstrated.

The paper is structured as follows. In Sec. II, the space-charge-Twiss modification in RDTs is demonstrated. In Sec. III, modified RDTs scheme and 2 additional schemes are used in the simulation to compensate for corresponding magnetic field errors during resonance crossing. The half-integer and 3rd-order resonance crossing are successfully compensated by the modified RDTs. Sec. IV contains a summary of the whole paper.

* Corresponding author.; yangjch@impcas.ac.cn

II. SPACE-CHARGE-TWISS MODIFICATION IN RDTs

RDTs, based on the description in normal forms of the beam oscillations, are quiet effective tools on nonlinear beam dynamics as shown in Eq. (1). According to RDTs, the horizontal TbT data of the complex Courant-Snyder variables at the location of the Beam Position Monitor (BPM), denoted as b , can be decomposed into a series of Fourier components[12]:

$$\begin{aligned} [\hat{x} - i\hat{p}_x](N, b) = & \sqrt{2I_x} e^{i(2\pi\nu_x N + \phi_{x_b})} \\ & - 2i \sum_{jklm} j f_{jklm}^{(b)} (2I_x)^{\frac{j+k-1}{2}} (2I_y)^{\frac{l+m}{2}} \\ & \times e^{i[(1-j+k)(2\pi\nu_x N + \phi_{x_b}) + (m-l)(2\pi\nu_y N + \phi_{y_b})]} \end{aligned} \quad (1)$$

where \hat{x} and \hat{p}_x are the normalized coordinates, $I_{x,y}$ are the nonlinear action-angle variables, and $\nu_{x,y}$ are the tunes influenced by detuning due to either linear coupling or amplitude dependent effects. The horizontal and vertical phase of the lattice at the BPM location b are denoted as ϕ_{x_b, y_b} . The resonance driving terms in Eq. (1), $f_{jklm}^{(b)}$, are :

$$f_{jklm}^{(b)} = \frac{\sum_{\omega} h_{\omega, jklm} e^{i[(j-k)\Delta\phi_{\omega, x}^b + (l-m)\Delta\phi_{\omega, y}^b]}}{1 - e^{2\pi i[(j-k)Q_x + (l-m)Q_y]}} \quad (2)$$

where the ω is the location of the ω^{th} multipole, the $\Delta\phi_{\omega, x, y}^b$ is the phase advance between the ω^{th} multipole and the location b , and the $h_{\omega, jklm}$ is:

$$\begin{aligned} h_{\omega, jklm} = & -\frac{\Omega_{\omega, n-1}(l+m)}{j!k!l!m!2^{j+k+l+m}} i^{l+m} (\beta_{\omega, x})^{\frac{j+k}{2}} (\beta_{\omega, y})^{\frac{l+m}{2}} \\ \Omega_{\omega, n-1}(l+m) = & \begin{cases} K_{\omega, n-1} L & \text{if } (l+m) \text{ is even} \\ iJ_{\omega, n-1} L & \text{if } (l+m) \text{ is odd} \end{cases} \end{aligned} \quad (3)$$

where n is the order of resonance, $n = j + k + l + m$, K is the normal multipole coefficient, J is the skew multipole coefficient and L is the length of the ω^{th} multipole. When space charge effect could be ignored, the RDTs are useful tools to study the effect of magnetic nonlinear fields in the betatron motion. Fig. (1) demonstrates a simple example of 3-order resonance compensation obtained by RDTs.

However, space charge is not included in RDTs. As a result, RDTs do not have a good performance on multipole-driven resonance compensation under space-charge-induced resonance crossing. In the following text, space charge would be introduced in order to study the combined effect of space charge and magnetic field imperfections.

When space charge could not be ignored, treating the space-charge potential U_{sc} as a perturbation, the Hamiltonian becomes:

$$H = \frac{p_x^2 + K_x x^2}{2} + \frac{p_y^2 + K_y y^2}{2} + U_{sc} \quad (4)$$

where the $K_{x,y}$ is the normalized quadrupole strength. For a

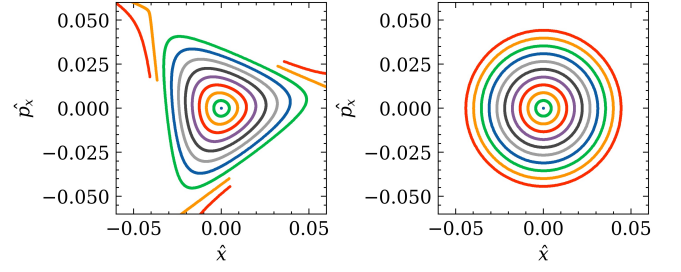


FIG. 1. The left subgraph shows the normalized phase space with a small sextupole error at $3Q_x = 28$. The right subgraph shows the normalized phase space with compensation obtained by RDTs. This simulation is constructed without space charge.

beam with bi-Gaussian charge distribution[13]:

$$U_{sc} = \frac{K_{sc}}{2} \int_0^\infty \frac{\exp[-\frac{x^2}{2\sigma_x^2+t} - \frac{y^2}{2\sigma_y^2+t}] - 1}{\sqrt{(2\sigma_x^2+t)(2\sigma_y^2+t)}} dt \quad (5)$$

where σ_u is the envelope radii, the K_{sc} is the ‘‘normalized’’ space-charge perveance parameter given by $K_{sc} = 2\lambda r_0 / (\beta_{rel}^2 \gamma_{rel}^3)$, where λ could be obtained by the bunch intensity N_B and the longitudinal rms bunch length σ_s , $\lambda = N_B / (\sqrt{2\pi}\sigma_s)$, r_0 is the particle classical radius $e^2 / (4\pi\epsilon_0 mc^2)$, β_{rel} and γ_{rel} are Lorentz factors. For particles with small amplitude at the center of the beam, Eq. (5) could be expanded in Taylor series, the first order of which demonstrates its linear defocusing quadrupole strength:

$$\frac{\partial U_{sc}}{\partial u} = -\frac{K_{sc}}{\sigma_u(\sigma_x + \sigma_y)} u + \dots = -K_{u,sc} u + \dots \quad (6)$$

where u presents x or y , $-K_{u,sc}$ presents the defocusing quadrupole strength introduced by space charge. Then the Hill equation becomes:

$$u'' + [K_u - K_{u,sc}]u = 0 \quad (7)$$

from which a new series of Twiss parameters influenced by space charge could be obtained, but they could only apply to particles with small amplitude. For particles with larger amplitudes, the absolute value of the defocusing quadrupole strength $-K_{u,sc}$ is smaller than Eq.(6), leading to a correspondingly smaller tune shift. This has been demonstrated by the *Poincaré* map in [14], the frequency map analysis in [15], and distribution density of the space-charge tune shift in [16]. In order to describe the betatron motion of all particles in a bunch, Eq. (7) could be rewritten in the form that depends on the action J_u of particles:

$$u'' + [K_u - K_{u,sc}(J_u)]u = 0 \quad (8)$$

Twiss parameters influenced by space charge of particles with any J_u could be obtained by Eq. (5-8). However, focusing on particles undergoing resonance crossing through Eq. (8) is complex. The primary objective of this paper is to compensate for resonance crossing, necessitating a focus on specific

particles whose tunes intersect resonance lines. The largest betatron tune shift for a beam with a bi-Gaussian charge distribution is given by [13]:

$$\Delta\nu_{sc,u} = -\frac{K_{sc}}{4\pi} \oint \frac{\beta_u}{\sigma_u(\sigma_x + \sigma_y)} ds \quad (9)$$

where the β_u is the original β function without space charge. Substituting Eq. (9) back into Eq. (6), the linear strength becomes the form that depends on the tune shift $\Delta\nu_{sc,u}$:

$$u'' + [K_u - K_{u,sc}(\Delta\nu_{sc,u})]u = 0 \quad (10)$$

which demonstrates that Twiss parameters influenced by space charge, $\beta_{u,sc}$ and phase $\phi_{u,sc}$, could be obtained by Eq. (10) through adjusting the value of $\Delta\nu_{sc,u}$. Then the Twiss of space-charge-influenced particles in the vicinity of resonance lines could be obtained. For other kinds of beam distribution, the Eq. (6,9) would change into corresponding form. But the Eq. (10) could always be established. So this approach could be applied to any beam distribution.

Replace the β_u and ϕ_u in RDTs with $\beta_{u,sc}$ and $\phi_{u,sc}$:

$$f_{ijklm}^{(b)}(\beta_u, \phi_u) \longrightarrow f_{ijklm}^{(b)}(\beta_{u,sc}, \phi_{u,sc}) \quad (11)$$

from which the space charge modification has been introduced into RDTs. The new RDTs are named modified RDTs, which could be used to compensate for magnetic field imperfections under space-charge-induced resonance crossing. This approach is the key idea of this paper, which is to obtain the new space-charge-influenced Twiss parameters to modify the RDTs. Note that the β_u in Eq. (3) should be replaced as well.

Here is an example on how to establish the modified RDTs compensation. Assuming that the chromaticity is 0, when a low-intensity beam is injected into the ring, the tune will be centered around the bare tune, $Q_x = 9.47, Q_y = 9.43$ in Fig. (2). As beam intensity increases, the tune spread enlarges until it hits the resonance line $3Q_y = 28$, shown as the orange tune spread in Fig. (2). The original skew sextupoles in the ring would cause a stop band at this resonance line, limiting further intensity increase. By applying Eq. (10, 11), the strength of the skew sextupole correctors can be determined to minimize the first group of modified RDTs $f_{0030}(\beta_{u,sc}, \phi_{u,sc})$ of the core particles, thereby mitigating the stop band and facilitating resonance crossing at $3Q_y = 28$. Then as the intensity keeps increasing, the largest tune shift would hit the resonance line $Q_x + 2Q_y = 28$, shown as the green tune spread in Fig. (2). By applying Eq. (10,11), the strength of the sextupole correctors can be calculated to minimize the second group of modified RDTs $f_{1020}(\beta_{u,sc}, \phi_{u,sc})$ of the core particles, facilitating resonance crossing at $Q_x + 2Q_y = 28$. At this stage, the first group of modified RDTs $f_{0030}(\beta_{u,sc}, \phi_{u,sc})$ now describes the nonlinear motion of larger-amplitude particles, rather than the core particles. This means the ignored space-charge-induced nonlinear force becomes stronger. According to the following simulation, the space-charge-induced nonlinear force would make Eq. (10) imprecise for halo particles[17] with large amplitude at the edge of the beam. In a word, this approach is precise for core particles but imprecise for halo

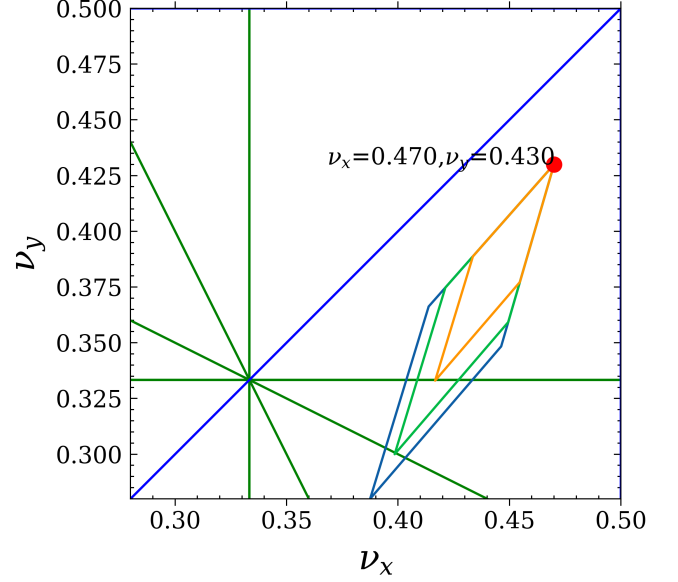


FIG. 2. This figure shows an example on how to establish the modified RDTs compensation. The orange and green rhombus represent the tune spreads which hit resonance lines. The integer part of the tune value cannot be obtained, so all tune maps use the decimal part as the coordinate axis.

particles, as the dynamics of halo particles is complicated for the nonnegligible nonlinearity at the edge of the beam. More examples of using Eq. (11) for compensation can be found in Sec. III.

III. SIMULATION

A. Systematic resonance analysis

Nonlinear resonances are classified into systematic and random resonances. Systematic nonlinear resonances are located at $\ell = P \times integer$, where P is the superperiod of an accelerator[18]. A systematic resonance would be hit even without magnet imperfections. A systematic resonance must be avoided, both in the simulation and in the reality. The

TABLE I. BRing parameters to test half-integer resonance crossing

Number of bunches	1
Kinetic energy	17MeV/nucleon
Tune (ν_x, ν_y)	(9.52, 9.43)
Intensity: ion num of $^{238}\text{U}^{35+}$	2×10^{10}
Simulation aperture	(300,150) π mm mrad
Injection RMS emittance (ϵ_x, ϵ_y)	(42.10, 14.06) π mm mrad
Transverse distribution	Gaussian truncated at 6σ
RMS bunch length σ_s	20.4m
Injection momentum spread δ	0.0015
Number of macroparticles	1×10^6
Max space charge tune shifts ($\Delta\nu_x, \Delta\nu_y$)	(0.05, 0.08)

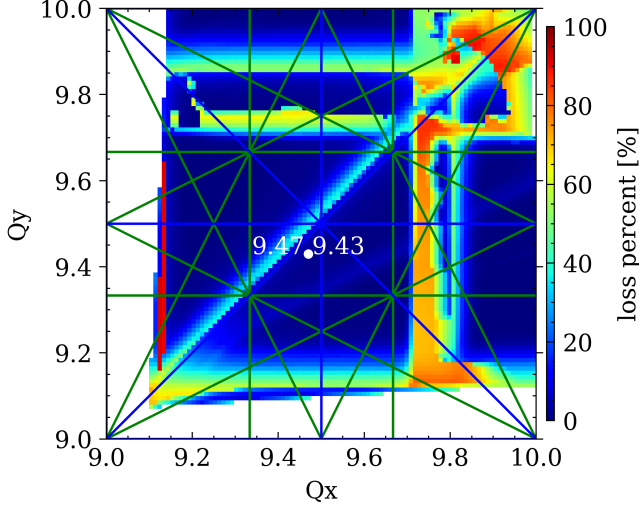


FIG. 3. The figure shows the simulation of HIAF-BRring tune scan map, where the white area has no data due to the unable tune matching. In the figure, the beam envelope is well matched to the aperture, which means any emittance growth would result in beam loss. The beam loss is shown by the color. This simulation is constructed without magnetic field imperfections.

analysis of systematic resonance in the HIAF-BRring lattice is shown in Fig. (3). As the analysis shows, even without magnetic field imperfections, systematic resonances would be hit at $4Q_x = 39$, $4Q_y = 39$, $8Q_x = 73$, $8Q_y = 73$, $8Q_y = 79$. Montague resonance driven by space charge would be hit at $2Q_x - 2Q_y = 0$. The tune of HIAF-BRring must locate away from these resonance lines.

B. Half-integer resonance crossing at $2Q_x = 19$

$2Q_x = 19$ is chosen because it does not correspond to a systematic resonance, as illustrated in Fig. (3). To investigate the half-integer resonance crossing at $2Q_x = 19$, the parameters of HIAF-BRring are adjusted as shown in Table I. To facilitate statistical analysis, the number of bunches is set to 1. Fig. (4) shows the corresponding tune spread map without chromaticity. 'Without chromaticity' means that quadrupoles would not introduce chromaticity in the simulation.

For modified RDTs, firstly, the raw Twiss parameters at (9.52,9.43) could be obtained by the 'TWISS' order of MAD-X[19], which could provide the raw betatron function β_u and phase ϕ_u . Second, since the tune spread would cross $Q_x = 9.5$, substituting $\Delta v_{sc,x} = (9.5 - 9.52 + o)$ (o asymptotically approaches zero to prevent the denominator of $f_{jklm}^{(b)}$ from going to zero.) into Eq. (10):

$$x'' + [K_x - K_{x,sc}(\Delta v_{sc,x} = 9.501 - 9.520)]x = 0 \quad (12)$$

where the additional 0.001 is the o . Third, get the corresponding $\beta_{x,sc}$ and $\phi_{x,sc}$ of space-charge-influenced particles which cross $Q_x = 9.5$ through Eq. (12). As shown in the bottom subgraph of Fig. (5), the tune obtained by Eq. (12) approx 9.5.

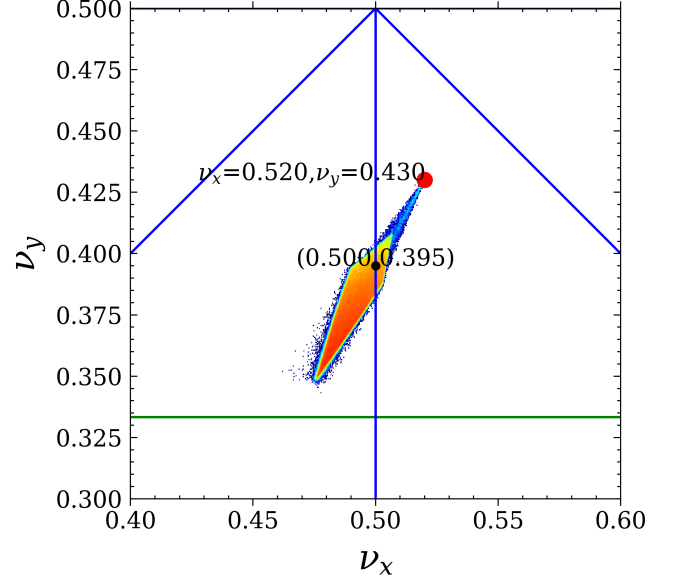


FIG. 4. The space charge tune spread using parameters in Table I without chromaticity, under the resonance crossing at $2Q_x = 19$. The black dot is one of the intersections of the tune spread and the resonance line, which could be used in Eq. (10).

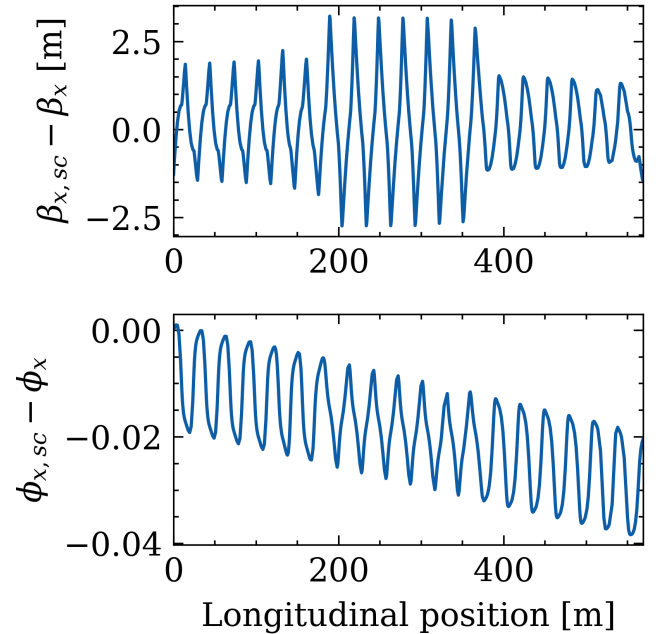


FIG. 5. This two subgraphs shows the horizontal Twiss differences between the new Twiss obtained by Eq. (12) and the original Twiss at (9.52,9.43).

Finally, use the new Twiss $\beta_{x,sc}$, $\phi_{x,sc}$, and Eq. (11) to get the modified RDTs along the ring:

$$f_{2000}(\beta_{x,sc}, \phi_{x,sc}) \quad (13)$$

The whole progress is recorded as:

$$\Delta v_{sc,x} = 9.501 - 9.520 \rightarrow f_{2000}(\beta_{x,sc}, \phi_{x,sc}) \quad (14)$$

Minimise the modified RDTs would achieve the compensation. The method to minimise the RDTs has been well established in the previous study. In a word, minimising RDTs is to introduce additional multipoles into the lattice with magnetic correctors for mitigating the original RDTs driven by corresponding multipoles due to various imperfections, including but not limit to alignment errors, rotation errors, and multipole errors in the magnet itself. Details on minimising RDTs could be found in [20, 21].

For (unmodified) RDTs, first get the Twiss parameters at (9.52,9.43) from MAD-X, $\beta_x(9.52, 9.43)$, $\phi_x(9.52, 9.43)$. Then, get RDTs directly through this Twiss and minimise the RDTs along the ring. In the later text, this scheme is called as raw RDTs:

$$f_{2000}(\beta_x(9.52, 9.43), \phi_x(9.52, 9.43)) \quad (15)$$

For another scheme, first adjust the tune into the vicinity of the half-integer resonance line (9.50+ ϵ ,9.39) through 'MATCH' order of MAD-X and get Twiss parameters, $\beta_x(9.501, 9.395)$, $\phi_x(9.501, 9.395)$. Then get RDTs through this Twiss and minimise the RDTs along the ring:

$$f_{2000}(\beta_x(9.501, 9.395), \phi_x(9.501, 9.395)) \quad (16)$$

Finally, match the tune back to (9.52,9.43) for simulation. In the later text, this scheme is called moved RDTs.

The key difference among these 3 schemes is the Twiss: modified RDTs use space-charge-influenced Twiss, raw RDTs use the Twiss at operating point (9.52,9.43), moved RDTs use the Twiss at the intersection of the tune spread and resonance lines through 'MATCH' order of MAD-X.

Fig. (6) shows the emittance evolution for each compensation scheme without chromaticity. The modified RDTs compensation scheme performs the best, demonstrating small emittance growth during the first 30 turns and negligible growth in the rest of the evolution. In contrast, the simulation without compensation shows rapid emittance growth during the initial 50 turns. The emittance growth then stabilizes between 50 and 1000 turns, as the reduced tune spread, resulting from beam loss and emittance increase, no longer intersects the half-integer resonance line.

Fig. (7) presents the normalized phase spaces, clearly illustrating the presence of resonance islands in the phase spaces with raw RDTs and moved RDTs. In contrast, the phase space with modified RDTs shows little resonance behavior. The stable resonance islands observed in the bottom two subgraphs are due to insufficient compensation. This phenomenon explains why the emittance with raw RDTs and moved RDTs stops growing at 600-1000 turns. The phase space without compensation is not shown, as the amplitude of each particle increases rapidly, leading to chaotic particle distribution with almost no useful information.

The Fig. (4-7) could be redrawn as Fig. (8) after introducing chromaticity into the simulation. As shown in the top left subgraph, chromaticity introduces an additional tune shift $\xi_u \delta$ to each particle, which varies with the longitudinal phase space oscillation. In the simulation, the Radio-Frequency(RF) cavity maintains a voltage of 65,000 V and

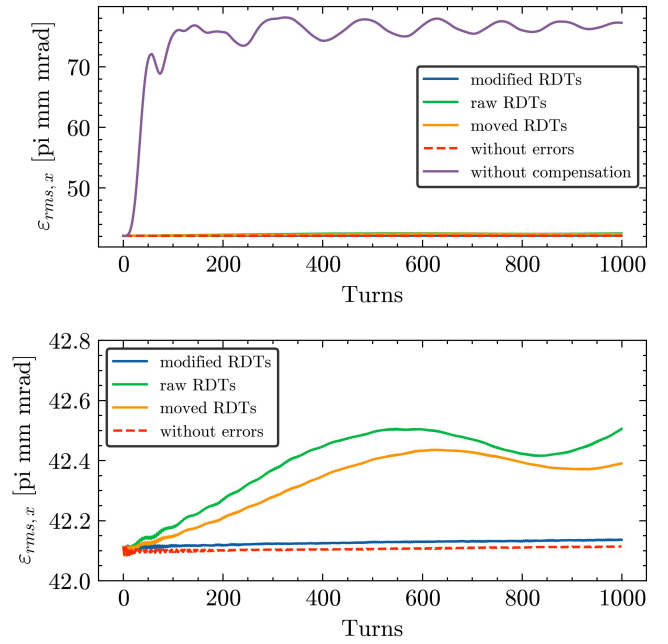


FIG. 6. The horizontal emittance evolution under the tune spread in Fig. (4). The quadrupole errors come from gaussian random values, $3\sigma(\Delta B_1/B_1) = 1 \times 10^{-3}$, on all quadrupoles. In the top subgraph, the emittance without compensation grows too much, causing that rest results almost overlap. The bottom subgraph shows more details about the comparison between these compensation schemes.

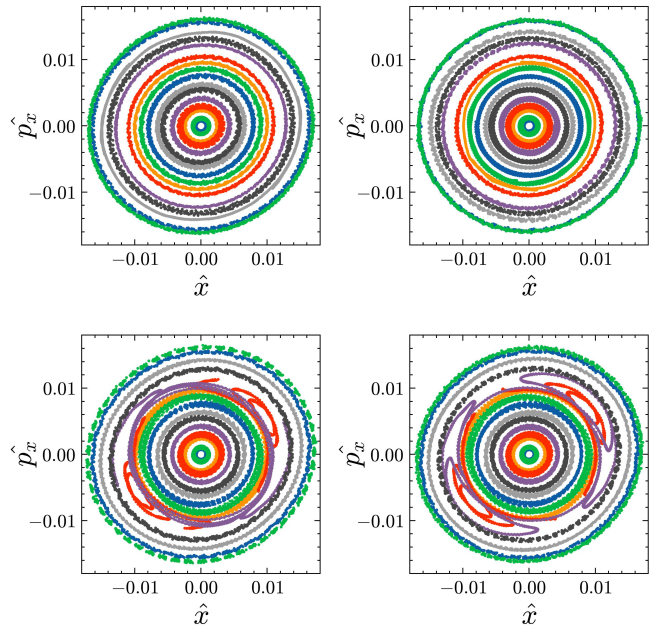


FIG. 7. The normalized phase spaces under the tune spread in Fig. (4). The top left subgraph shows the phase space without errors. The top right subgraph shows that with modified RDTs. The bottom left subgraph shows that with raw RDTs. The bottom right subgraph shows that with moved RDTs. In the unshown phase space without compensation, which is a mess, the amplitude of almost each particle grows rapidly.

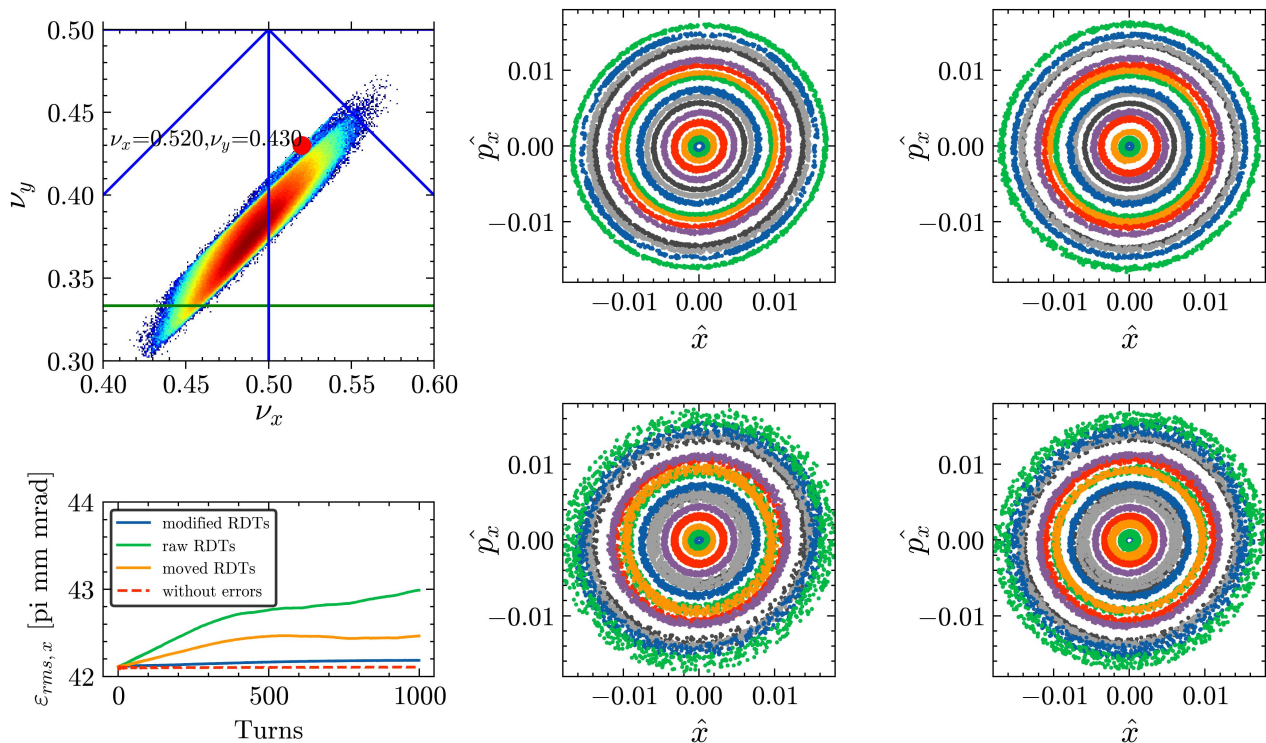


FIG. 8. The left top subgraph shows space charge tune spread using parameters in Table I with chromaticity. The left bottom subgraph shows the bottom subgraph in Fig. (6) with chromaticity. The right 4 subgraphs show Fig. (7) with chromaticity.

a phase of 0 for the ideal particle. The synchrotron tune is approximately 0.00625. After introducing chromaticity, the emittance growth for each compensation scheme becomes larger. The modified RDTs scheme still has the best performance but its emittance also grows slowly compared to the results shown in Fig. (6). This increase may be attributed to the neglect of chromaticity effects in the modified RDTs. In the right 4 subgraphs, resonance islands are no longer present, but oscillation distortions can be observed in the bottom two subgraphs. Comparing the phase space with the modified RDTs scheme to that without errors, it can be seen that the amplitude of the particles with the modified RDTs scheme varies slightly, but the phase space remains consistent with the ideal case. This confirms the successful compensation for half-integer resonance crossing using the modified RDTs scheme.

In this section, the compensation for the half-integer resonance crossing at $2Q_x = 19$ through the 3 different compensation schemes is demonstrated. The compensation scheme with modified RDTs has the best performance. In conclusion, the feasibility of half-integer resonance crossing compensation by modified RDTs is confirmed by the simulation.

C. 3rd-order resonance crossing

In this section, the parameters of HIAF-BRing in the simulation are presented in Table II. To facilitate statistical analysis, the number of bunches is also set to 1. The corresponding

tune spread without chromaticity is shown in Fig. (9). In the simulation of complete acceleration, where the beam transitions from a coasting beam to being captured and accelerated from 17 to 835 MeV/nucleon, the maximum space-charge-incoherent tune spread, $(\Delta v_{sc,x}, \Delta v_{sc,y})_{max} \approx (0.16, 0.28)$, is smaller than that in Fig. (9). This discrepancy arises from differences in kinetic energy and longitudinal beam distribution. At the moment space-charge-incoherent tune spread reaches its maximum, firstly the kinetic energy has increased to 17.65 MeV/nucleon rather than the injection kinetic energy of 17 MeV/nucleon. Secondly, longitudinal distribution formed during the capture and acceleration differs from the program-generated longitudinal distribution. This shows that the space-charge-induced tune spread in this simulation is large enough.

As Fig. (9) shows, the tune spread crosses five 3rd-order resonance lines, $3Q_y = 28$, $2Q_x + Q_y = 28$ driven by skew sextupoles and $3Q_x = 28$, $Q_x + 2Q_y = 28$, $Q_x - 2Q_y = -9$ driven by normal sextupoles. With the aperture set to the designed (200,100) π mm mrad, 30% of the beam would be lost in the simulation of complete acceleration while sextupole and skew sextupole errors are introduced. The 3rd-order resonance crossing is a significant problem that limits the intensity of HIAF-BRing. For modified RDTs, 5 groups of modified RDTs should be obtained through the black dots by Eq. (10-

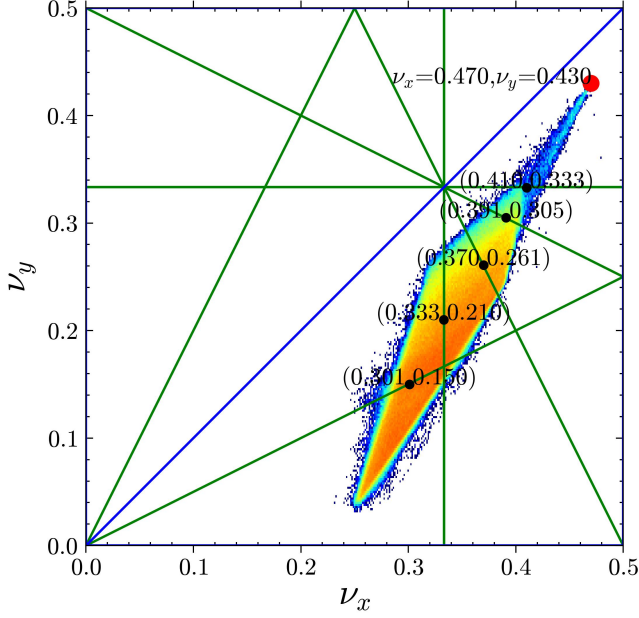


FIG. 9. The tune spread without chromaticity using parameters in Table II, where resonance crossing is hit at $3Q_x = 28$, $Q_x + 2Q_y = 28$, $Q_x - 2Q_y = -9$ driven by sextupole errors and $3Q_y = 28$, $2Q_x + Q_y = 28$ driven by skew sextupole errors. The black dots are intersections of the tune spread and resonance lines, which could be used in Eq. (10).

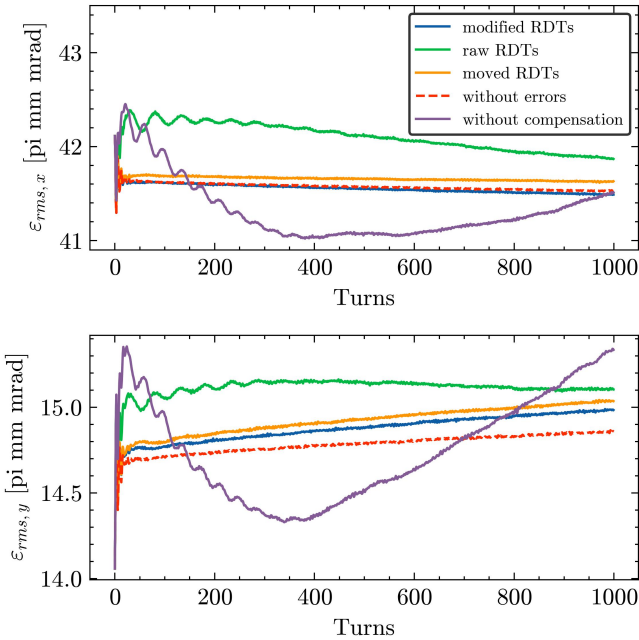


FIG. 10. The emittance evolution under the tune spread in Fig. (9). The sextupole and skew sextupole errors come from $3\sigma(\Delta B_2/B_1) = 1 \times 10^{-3}$ of all quadrupoles.

TABLE II. BRing parameters to test 3rd-order resonance crossing

Number of bunches	1
Kinetic energy	17MeV/nucleon
Tune (ν_x, ν_y)	(9.47, 9.43)
Intensity: ion num of $^{238}\text{U}^{35+}$	1×10^{11}
Simulation aperture	(300, 150) π mm mrad
Injection RMS emittance (ϵ_x, ϵ_y)	(42.10, 14.06) π mm mrad
Transverse distribution	Gaussian truncated at 6σ
RMS bunch length σ_s	20.4m
Injection momentum spread δ	0.0015
Number of macroparticles	1×10^6
Max space charge tune shifts ($\Delta\nu_x, \Delta\nu_y$)	(0.22, 0.40)

11):

$$\begin{aligned}
 & \begin{cases} \Delta\nu_{sc,x} = 9.420 - 9.47 \\ \Delta\nu_{sc,y} = 9.333 - 9.43 \end{cases} \rightarrow f_{0030}(\beta_{u,sc}, \phi_{u,sc}) \\
 & \begin{cases} \Delta\nu_{sc,x} = 9.401 - 9.47 \\ \Delta\nu_{sc,y} = 9.300 - 9.43 \end{cases} \rightarrow f_{1020}(\beta_{u,sc}, \phi_{u,sc}) \\
 & \begin{cases} \Delta\nu_{sc,x} = 9.370 - 9.47 \\ \Delta\nu_{sc,y} = 9.261 - 9.43 \end{cases} \rightarrow f_{2010}(\beta_{u,sc}, \phi_{u,sc}) \quad (17) \\
 & \begin{cases} \Delta\nu_{sc,x} = 9.333 - 9.47 \\ \Delta\nu_{sc,y} = 9.210 - 9.43 \end{cases} \rightarrow f_{3000}(\beta_{u,sc}, \phi_{u,sc}) \\
 & \begin{cases} \Delta\nu_{sc,x} = 9.301 - 9.47 \\ \Delta\nu_{sc,y} = 9.150 - 9.43 \end{cases} \rightarrow f_{1002}(\beta_{u,sc}, \phi_{u,sc})
 \end{aligned}$$

where the 5 groups of modified RDTs should be minimised by corresponding correctors. For raw RDTs, just get 5 groups of RDTs at (9.47, 9.43) and minimise them. For moved RDTs, match the tune to the 5 black dots in Fig. (9). Corresponding groups of RDTs should be obtained at each tune. Minimise the RDTs and match the tune back to (9.47, 9.43) for simulation.

Fig. (10) shows the emittance evolution without chromaticity of each compensation scheme. The Montague resonance[22] has a small influence on the beam, leading to a weak action transfer from the horizontal to the vertical plane even in the absence of magnetic field errors. The compensation scheme of modified RDTs demonstrates the best performance. For modified RDTs, the $\epsilon_{rms,x}$ keeps the same as that without errors, and the $\epsilon_{rms,y}$ grows by 2%, due to the insufficient compensation for halo particles at $3Q_y = 28$. It can be observed that the statistical RMS emittance without compensation and with raw RDTs increases in the initial 20 turns, and decreases in the rest of the evolution. In fact the emittance of the beam keeps increasing, but particles at edge of the beam reach the simulation aperture, leading to the decrease of statistical RMS emittance.

The normalized phase spaces without errors, with modified RDTs and with moved RDTs are demonstrated in Fig. (11). In phase space without errors, the variable J_y and ν_y of the halo particles could be observed, leading to imprecise results of Eq. (10). The vertical oscillation of large amplitude particle is magnified due to space charge. As a result, the envelope radii in the vertical plane exceed the designed aperture even without imperfections, leading to 3.5% of the beam being lost during acceleration when the aperture is set to the designed (200, 100)

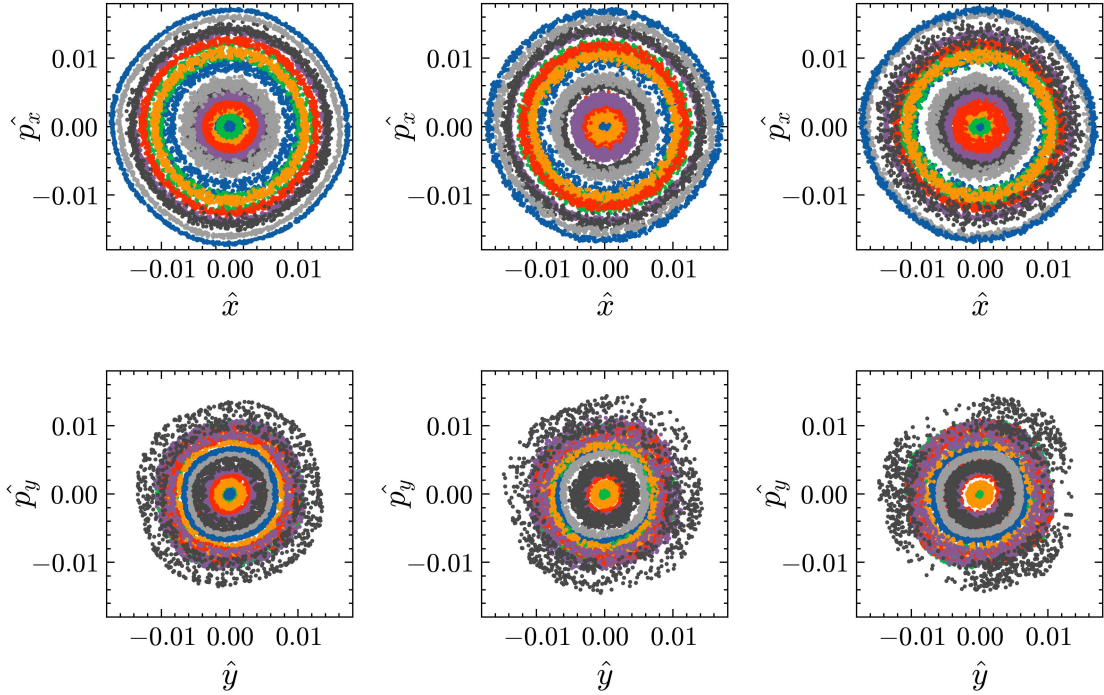


FIG. 11. The normalized phase spaces under the tune spread in Fig. (9). The left 2 subgraphs show the phase space without errors. The middle 2 subgraphs show that with modified RDTs. The right 2 subgraphs show that with moved RDTs.

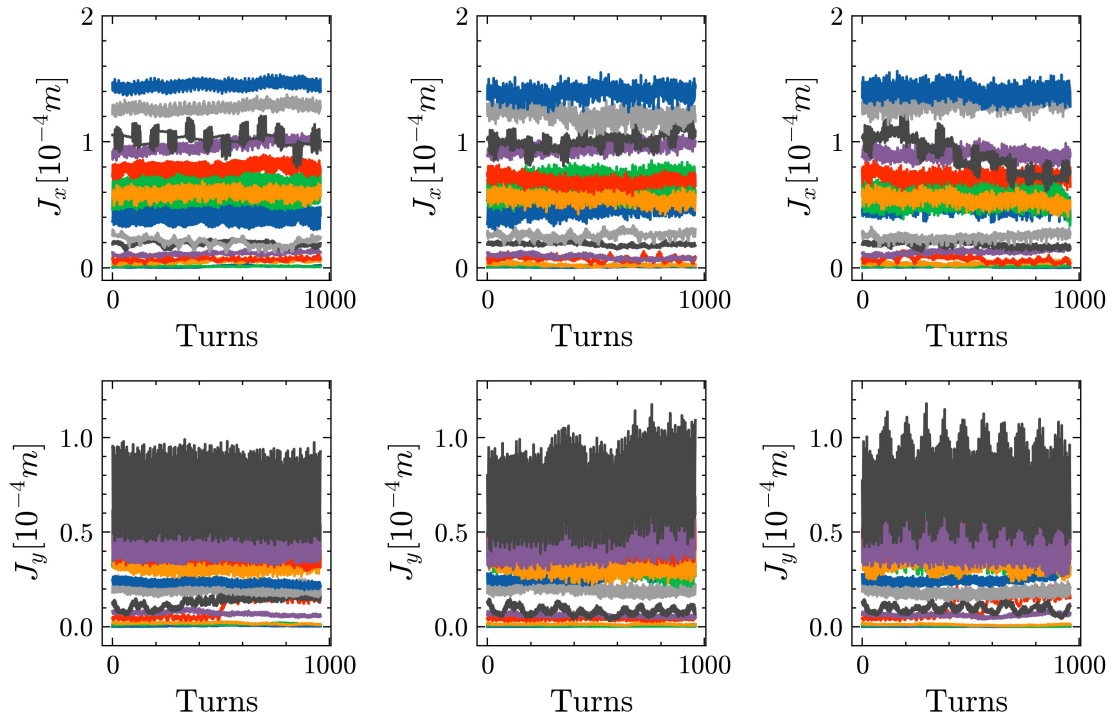


FIG. 12. The action in Fig. (11). The left 2 subgraphs show the phase space without errors. The middle 2 subgraphs show that with modified RDTs. The right 2 subgraphs show that with moved RDTs.

π mm mrad. In the phase space with modified RDTs, oscillation distortion could be observed in the horizontal plane but the RMS emittance remains almost the same as that without errors. A slight $3Q_y = 28$ resonance behavior on the black halo particle could be observed in the vertical plane, demonstrating the imprecise compensation for halo particles with modified RDTs. In the phase space with moved RDTs, the amplitude growth of the grey halo particle, the serious oscillation distortion of black halo particle in the horizontal plane and an obvious $3Q_y = 28$ resonance behavior of the black halo particle in the vertical plane could be observed. Note that the black halo particle in the horizontal plane and the black halo particle in the vertical plane are not the same one particle.

The oscillation of the phase space in Fig. (11) is not as clear as that in Fig. (7). An additional Fig. (12) is introduced to demonstrate the evolution of the action of particles in Fig. (11). For the result with modified RDTs, although its horizontal RMS emittance is almost the same as that without errors, its actions are not. For example, in the middle top subgraph of Fig. (12), the actions of the red particle whose initial J_x is 0.8×10^{-4} m and the orange particle whose initial J_x is 0.7×10^{-4} m decrease while the actions of the green particle whose initial J_x is 0.6×10^{-4} m and the blue particle whose initial J_x is 0.5×10^{-4} m increase. In the middle bottom subgraph, the action of the black halo particle becomes similar to that in the right bottom subgraph after 650 turns, which causes the "slight" $3Q_y = 28$ resonance behavior in the middle bottom subgraph in Fig. (11). In the initial 650 turns, this particle does not hit the stop band of $3Q_y = 28$. As the vertical emittance increases, the vertical space charge effect and the tune spread decreases. So this particle hit the stop band and is locked in the resonance islands in the rest of the evolution. For the result with moved RDTs, the stop band is larger than that with modified RDTs. As a result, the black halo particle is locked in the resonance islands in the beginning. Note that particles with the same color in the horizontal or vertical plane are the same particles.

The Fig. (9-12) could be redrawn into Fig. (13-16) after introducing chromaticity in the simulation. In Fig. (13), the chromaticity introduces an extra tune shift $\xi_u \delta$ to each particle, the same as seen in the left top subgraph in Fig. (8). In Fig. (14), for the result without compensation, the beam loss is rapid, causing the statistical $\epsilon_{rms,x}$ to decrease. Conversely, the ϵ_y grows rapidly, resulting in an increase in statistical $\epsilon_{rms,y}$ despite the beam loss. For the result with raw RDTs, emittance growth could be observed in both horizontal and vertical planes, indicating that the compensation scheme with raw RDTs is not effective under space-charge-induced resonance crossing. For the result with modified RDTs, the $\epsilon_{rms,x}$ is almost the same as that without errors, and the $\epsilon_{rms,y}$ grows by 2.5%, which is 0.5% larger than growth observed in Fig. (10). In Fig. (15), for the phase space with modified RDTs, the amplitude of the black halo particle becomes even smaller than that without errors. Fig. (17) demonstrates the J_u evolution of this particle, showing that there is no action transfer from the vertical to the horizontal plane. This phenomenon is interesting as the mechanism behind this action decrease under the combined effect of space charge, chromaticity, sextupole er-

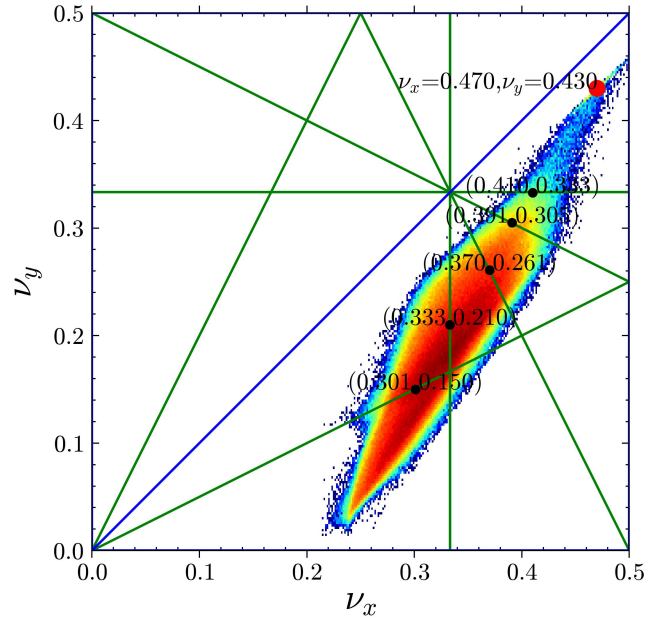


FIG. 13. The tune spread with chromaticity using parameters in Table II.

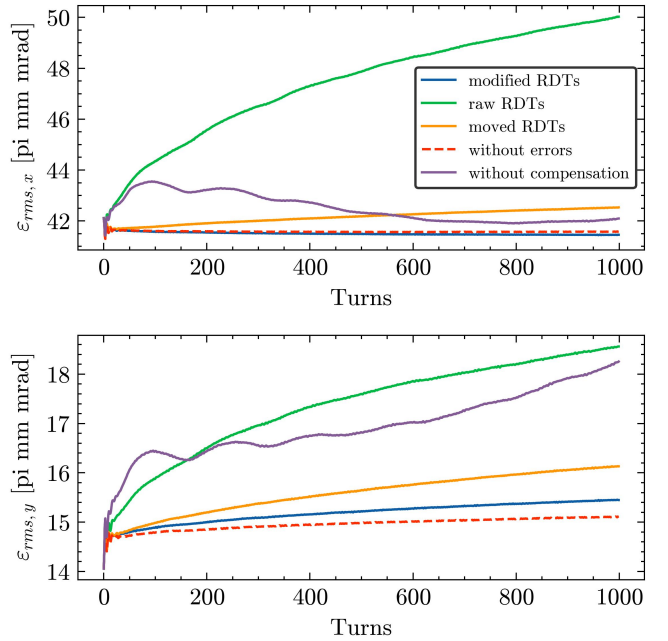


FIG. 14. The emittance evolution under the tune spread in Fig. (13).

rors and corresponding compensation is unclear and warrants further study.

In this section, the compensation for 3rd-order resonance crossing through 3 compensation schemes is demonstrated, using parameters in Table II. Despite the imperfect compensation for the halo particles, the compensation scheme with modified RDTs shows the best performance. In conclusion, the feasibility of 3rd-order resonance crossing compensated

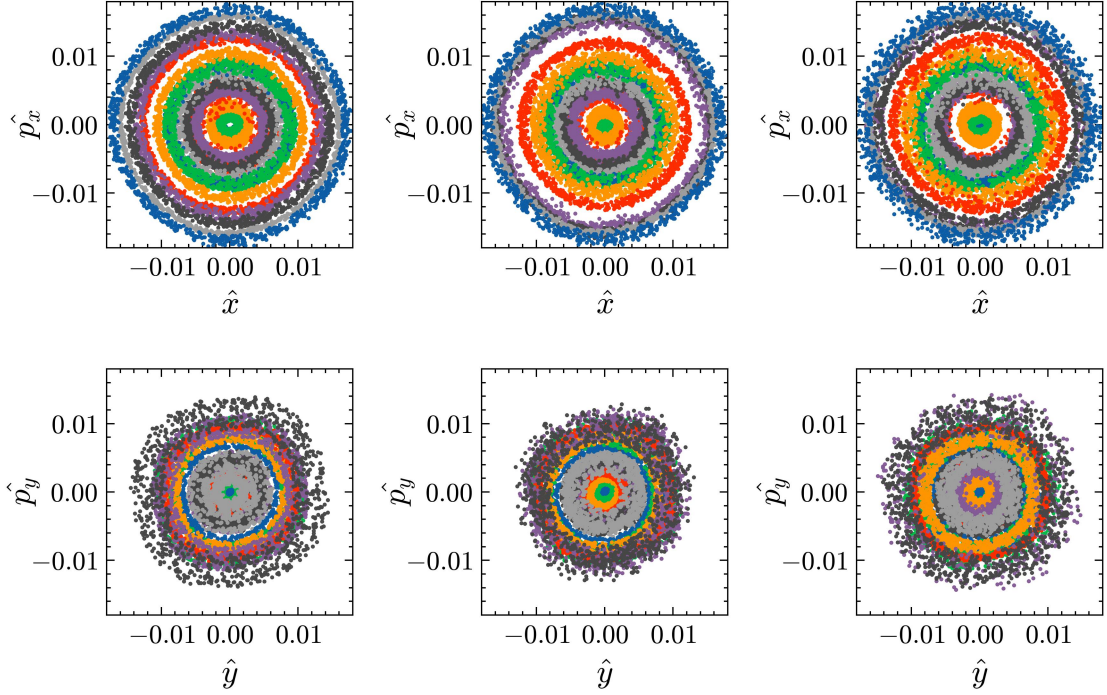


FIG. 15. The normalized phase spaces under the tune spread in Fig. (13). The left 2 subgraphs show the phase space without errors. The middle 2 subgraphs show that with modified RDTs. The right 2 subgraphs show that with moved RDTs.

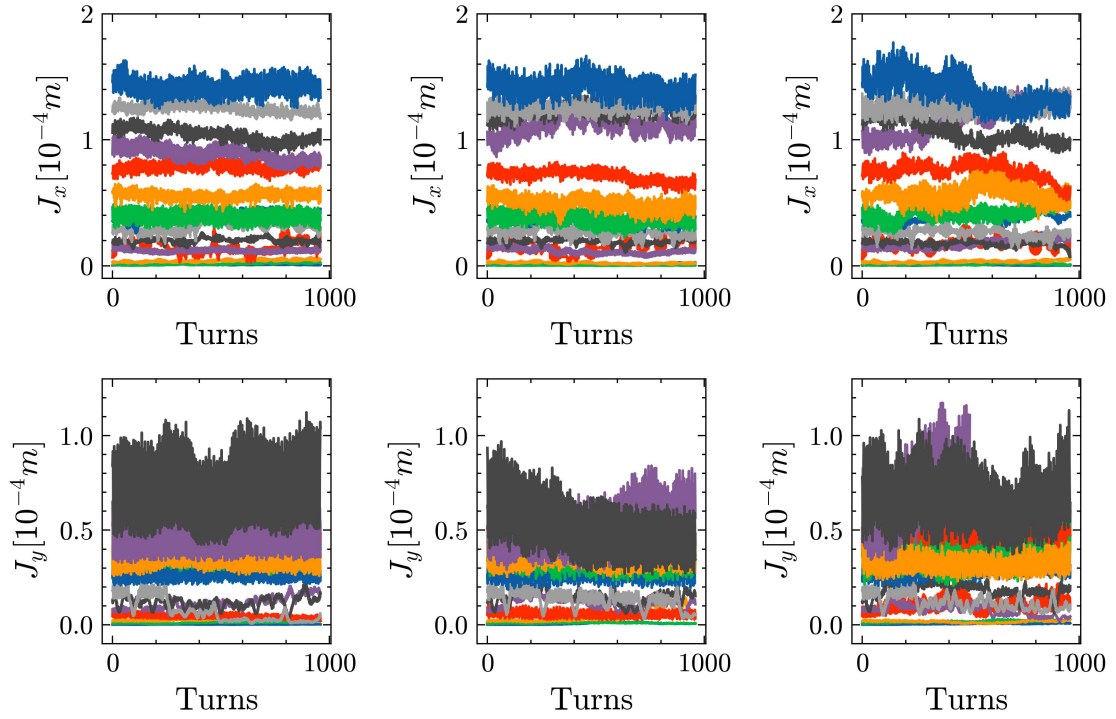


FIG. 16. The action in Fig. (15). The left 2 subgraphs show the phase space without errors. The middle 2 subgraphs show that with modified RDTs. The right 2 subgraphs show that with moved RDTs.

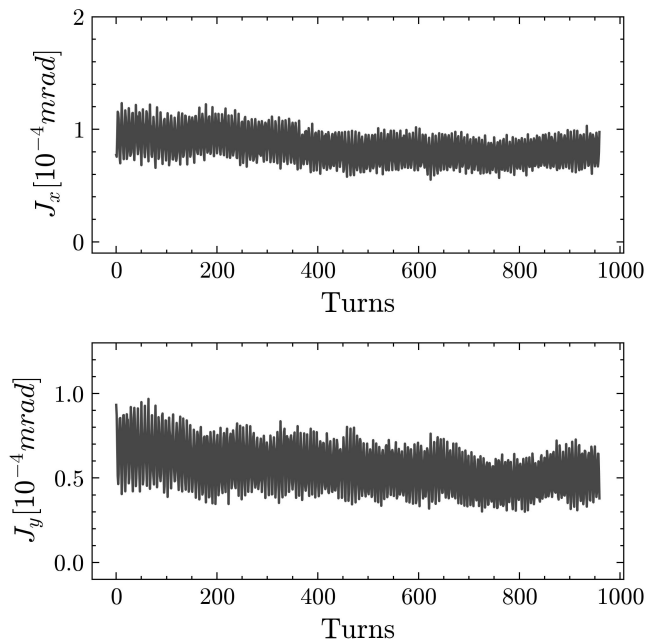


FIG. 17. The J_u evolution of the black halo particle in the middle bottom subgraph of Fig. (15).

by modified RDTs is confirmed by the simulation.

IV. CONCLUSIONS

In this paper, the key idea is to propose the space-charge-Twiss modification in RDTs, called modified RDTs. The modification is an approximate approach to obtain the Twiss

of particles under the space-charge-induced resonance crossing, through which the modified RDTs could be obtained. The modified RDTs aim to compensate for the combined effect of space charge and magnetic field imperfections, focusing on particles under resonance crossing. This approach is precise for core particles but imprecise for halo particles.

The feasibility of half-integer and 3rd-order resonance crossing compensated by modified RDTs is confirmed by the simulation, in which the raw RDTs and moved RDTs are also demonstrated for comparison. Among these schemes, the modified RDTs exhibits the best performance. The simulations are conducted both with and without chromaticity. The chromaticity has little influence on the overall compensation with modified RDTs, as evidenced by the almost unchanged RMS emittance evolution.

The modified RDTs scheme would be useful for any high-intensity accelerator, as it enables the compensation for the magnetic field imperfections under space-charge-induced resonance crossing. Magnetic correctors could be strategically placed at the appropriate phases in the lattice. By minimizing the modified RDTs with these correctors, the beam loss imposed by space-charge-induced resonance crossing can be mitigated. For HIAF-BRing, 26% of the beam loss, caused by the combined effect of space-charge-induced incoherent tune spread and magnetic field imperfections, could be prevented by the scheme of modified RDTs.

ACKNOWLEDGMENTS

This work was supported by ...

-
- [1] H. Bartosik, F. Asvesta, A. Huschauer, Y. Papaphilippou, and F. Schmidt, Space charge induced losses in the cern injector complex, *Journal of Instrumentation* **15** (07), P07021.
- [2] A. Oeftiger and O. Boine-Frankenheim, Pulsed electron lenses for space charge mitigation, *Physical Review Letters* **132**, 175001 (2024), pRL.
- [3] H. Hotchi, H. Harada, N. Hayashi, M. Kinsho, K. Okabe, P. Saha, Y. Shobuda, F. Tamura, K. Yamamoto, and M. Yamamoto, J-parc 3-gev rcs: 1-mw beam operation and beyond, *Journal of Instrumentation* **15** (07), P07022.
- [4] T. Yasui, S. Igarashi, Y. Sato, Y. Kurimoto, T. Shimogawa, Y. Morita, K. Ohmi, and T. Koseki, Compensations of third-order resonances in j-parc mr, in *Proceedings of the 12th International Particle Accelerator Conference, IPAC-2021, Campinas, SP, Brazil*.
- [5] A. S. García, F. Antoniou, S. Albright, F. Asvesta, H. Bartosik, G. Di Giovanni, B. Mikulec, and H. Rafique, Identification and compensation of betatronic resonances in the proton synchrotron booster at 160 mev, in *Proc. 10th Int. Particle Accelerator Conf. (IPAC'19)*, pp. 1054–1057.
- [6] F. Asvesta, F. Antoniou, S. Albright, C. Bracco, T. Prebibaj, G. P. Di Giovanni, E. Renner, E. Maclean, H. Bartosik, and B. Mikulec, Resonance compensation for high intensity and high brightness beams in the cern psb, *JACoW HB* **2021**, 40 (2022).
- [7] A. Bazzani, G. Servizi, G. Turchetti, and E. Todesco, *A normal form approach to the theory of nonlinear betatronic motion* (CERN, 1994).
- [8] A. Bazzani, P. Mazzanti, G. Servizi, and G. Turchetti, Normal forms for hamiltonian maps and nonlinear effects in a particle accelerator, *Il Nuovo Cimento B Series 11* **102**, 51 (1988).
- [9] F. Asvesta and H. Bartosik, Resonance driving terms from space charge potential, (2019).
- [10] J. Liu, J. Yang, J. Xia, D. Yin, G. Shen, P. Li, H. Zhao, S. Ruan, and B. Wu, Cisp: simulation platform for collective instabilities in the bring of hiaf project, *Nuclear Instruments and Methods in Physics Research Section A: Accelerators, Spectrometers, Detectors and Associated Equipment* **881**, 36 (2018).
- [11] X. Zhou, J. Yang, and H. P. Team, Status of the high-intensity heavy-ion accelerator facility in china, *AAPPS Bulletin* **32**, 35 (2022).
- [12] A. Franchi, L. Farvacque, F. Ewald, G. Le Bec, and K. B. Scheidt, First simultaneous measurement of sextupolar and octupolar resonance driving terms in a circular accelerator from turn-by-turn beam position monitor data, *Physical Review Special Topics - Accelerators and Beams* **17**, 10.1103/physrevstab.17.074001 (2014).
- [13] S. Y. Lee, G. Franchetti, I. Hofmann, F. Wang, and L. Yang,

- Emittance growth mechanisms for space-charge dominated beams in fixed field alternating gradient and proton driver rings, *New Journal of Physics* **8**, 291 (2006).
- [14] T. Yasui and Y. Kurimoto, Suppression of the eighth-order space-charge-induced resonance, *Physical Review Accelerators and Beams* **25**, 121001 (2022).
- [15] F. Asvesta, H. Bartosik, S. Gilardoni, A. Huschauer, S. Machida, Y. Papaphilippou, and R. Wasef, Identification and characterization of high order incoherent space charge driven structure resonances in the cern proton synchrotron, *Physical Review Accelerators and Beams* **23**, 091001 (2020), pRAB.
- [16] K. Y. Ng, Distribution of incoherent space-charge tune shift of bi-gaussian beam [10.2172/825289](#) (2004).
- [17] T. P. Wangler, Emittance growth from space-charge forces, *AIP Conference Proceedings* **253**, 21 (1992).
- [18] S.-Y. Lee, *Accelerator physics* (World Scientific Publishing Company, 2018).
- [19] H. Grote and F. Schmidt, Mad-x-an upgrade from mad8, in *Proceedings of the 2003 Particle Accelerator Conference*, Vol. 5 (IEEE) pp. 3497–3499.
- [20] E. Waagaard, Developing a resonance correction scheme in the lhc (2021).
- [21] F. S. Carlier, *A Nonlinear Future-Measurements and corrections of nonlinear beam dynamics using forced transverse oscillations* (Amsterdam U., 2020).
- [22] A. Oeftiger, O. Boine-Frankenheim, V. Chetvertkova, V. Kornilov, D. Rabusov, and S. Sorge, Simulation study of the space charge limit in heavy-ion synchrotrons, *Physical Review Accelerators and Beams* **25**, 054402 (2022), pRAB.